Synthesis of Organic−Inorganic Hybrid Gels from Siloxane or Silsesquioxane and α,ω-Nonconjugated Dienes by Means of a Photo Hydrosilylation Reaction

Naofumi Naga,*,† Yuki Kihara,† Tomoharu Miyanaga,† and Hidemitsu Furukawa‡

Department of Applied Chemistry, Materials Science Course, College of Engineering, Shibaura Institute of Technology, 3-7-5 Toyosu, Kohtoh-ku, Tokyo 135-8548, Japan, and Department of Biological Sciences, Graduate School of Science, Hokkaido University, N10, W8, Kita-ku, Sapporo 060-0810, Japan

Received April 25, 2008; Revised Manuscript Received March 24, 2009

ABSTRACT: Organic−inorganic hybrid gels have been synthesized from the multifunctional cyclic siloxane, 1,3,5,7-tetramethylcyclotetrasiloxane (TMCTS), or the cubic silsesquioxane, 1,3,5,7,9,11,13,15-octakis(dimethylsilyloxy)pentacyclo-[9,5,1,1,1,1]octasilsesquioxane (POSS), as cross-linking reagents with α,ω-nonconjugated dienes, 1,5-hexadiene (HD) or 1,9-decadiene (DD), using a photo hydrosilylation reaction with a bis(acetylacetonato)platinum catalyst in toluene. Network structures of the resulting gels, mesh size, and mesh size distribution were quantitatively characterized by means of a novel scanning microscopic light scattering (SMILS). The effects of the monomer concentration in the resulting gels were investigated, and gels with homogeneous network structure formed by 1.4 to 1.6 nm size of mesh were obtained under the monomer concentrations that are relatively higher than the critical gelation concentration. The mesh sizes of gels, that were determined with SMILS, with DD were larger than those with HD and were independent of the nature of the cross-linking reagents. The TMCTS-HD gel formation process was successfully traced with SMILS. The result indicates the formation of microgels in the early stages of the reaction following aggregation of the microgels, extension of the microgels, or both to form the infinite network that occupies the space of the reaction system around the gelation point. Photo-pattern coating of a glass plate with the POSS-DD gel was achieved by means of the photo hydrosilylation reaction of the cast reaction medium.

Introduction

Organic−inorganic hybrid polymers usually have characteristics derived from both the organic and inorganic components. Various types of organic−inorganic hybrid polymers that contain Si have been synthesized by a variety of synthetic methods including condensation reaction, hydrosilylation, and so on.[1−13] Hydrosilylation of multifunctionalized cross-linking reagents containing Si−H or vinyl groups is one useful method for synthesizing organic−inorganic hybrid polymers having network structures.[14−31] We think that the precise control of the network structures and the fundamental characterization of the organic−inorganic hybrid gel is essential not only to improve properties but also to develop novel network polymers with specific features. The authors recently developed organic−inorganic hybrid gels by means of hydrosilylation of a cyclic siloxane or a cubic silsesquioxane with α,ω-nonconjugated dienes using a highly efficient hydrosilylation catalyst, platinum−divinyltetramethyldisiloxane complex (Karstedt's catalyst), and quantitatively characterized the network structures of the gels by means of a characteristic analytical method, namely, scanning microscopic light scattering (SMILS).[32,33] In a previous investigation, we synthesized organic−inorganic hybrid gels having homogeneous network structure with controlled mesh sizes ranging from 0.5 to 5 nm by means of the hydrosilylation reaction between tetrafunctional cyclic siloxane (1,3,5,7-tetramethylcyclotetrasiloxane, TMCTS) and 1,5-hexadiene (HD) or 1,7-octadiene (Scheme 1).[32] The gels with expected network structures were prepared under the limited reaction conditions of the monomer and catalyst concentration. The concentration of the catalyst is one of the important factors in producing the gels with homogeneous network structure. When the reaction was conducted with high concentrations of Karstedt's catalyst, the heat of the reaction sometimes caused cracks or bubbles in the gels, resulting in inhomogeneity of network structure. Rapid diffusion of the catalyst is necessary for simultaneous reaction throughout the system when the catalyst is introduced to the reactor. With all precise investigations to find the optimal conditions, homogeneous mesh size distribution in the gels with large molecular nonconjugated diene, 1,9-decadiene (DD), or octafunctional cubic silsesquioxane, 1,3,5,7,9,11,13,15-octakis(dimethylsilyloxy)pentacyclo-[9,5,1,1,1,1]octasilsesquioxane (POSS), was not achieved with Karstedt's catalyst.[32] Therefore, we focused on another hydrosilylation catalyst that starts the reaction with a light, namely, "photo hydrosilylation".[34−36] UV irradiation to bis(acetylacetonato) platinum ($Pt(acac)_2$) catalyst induces hydrosilylation efficiently. We came up with an idea to use this photo hydrosilylation for the synthesis of the present organic−inorganic hybrid gels. In this study, we have investigated the synthesis of organic−inorganic hybrid gels from TMCTS or POSS with α,ω-nonconjugated dienes, HD or DD, by means of a hydrosilylation reaction with $Pt(acac)_2$ using UV irradiation, as shown in Scheme 2. The effect of the monomer concentration or monomer structure on the network structures in the gel was evaluated with SMILS. We have traced the reaction of TMCTS and HD with SMILS and studied the formation mechanism of the TMCTS-HD gel. We have also tried photo-pattern coating of a glass plate with the POSS-DD gel.

Experimental Part

Materials. HD and DD (Tokyo Kasei Kogyo) were distilled over calcium hydride under a nitrogen atmosphere. TMCTS (Chisso) and POSS (Aldrich Chemical), illustrated in Scheme 2, were used

* Corresponding author. E-mail: nnaga@sic.shibaura-it.ac.jp. Fax: +81-3-5859-8101.
† Shibaura Institute of Technology.
‡ Hokkaido University.

10.1021/ma802745x CCC: $40.75
Published on Web 04/21/2009

Scheme 1. Synthesis of Organic−Inorganic Hybrid Gels from TMCTS and POSS with HD and DD Using a Hydrosilylation Reaction with Karstedt's Catalyst

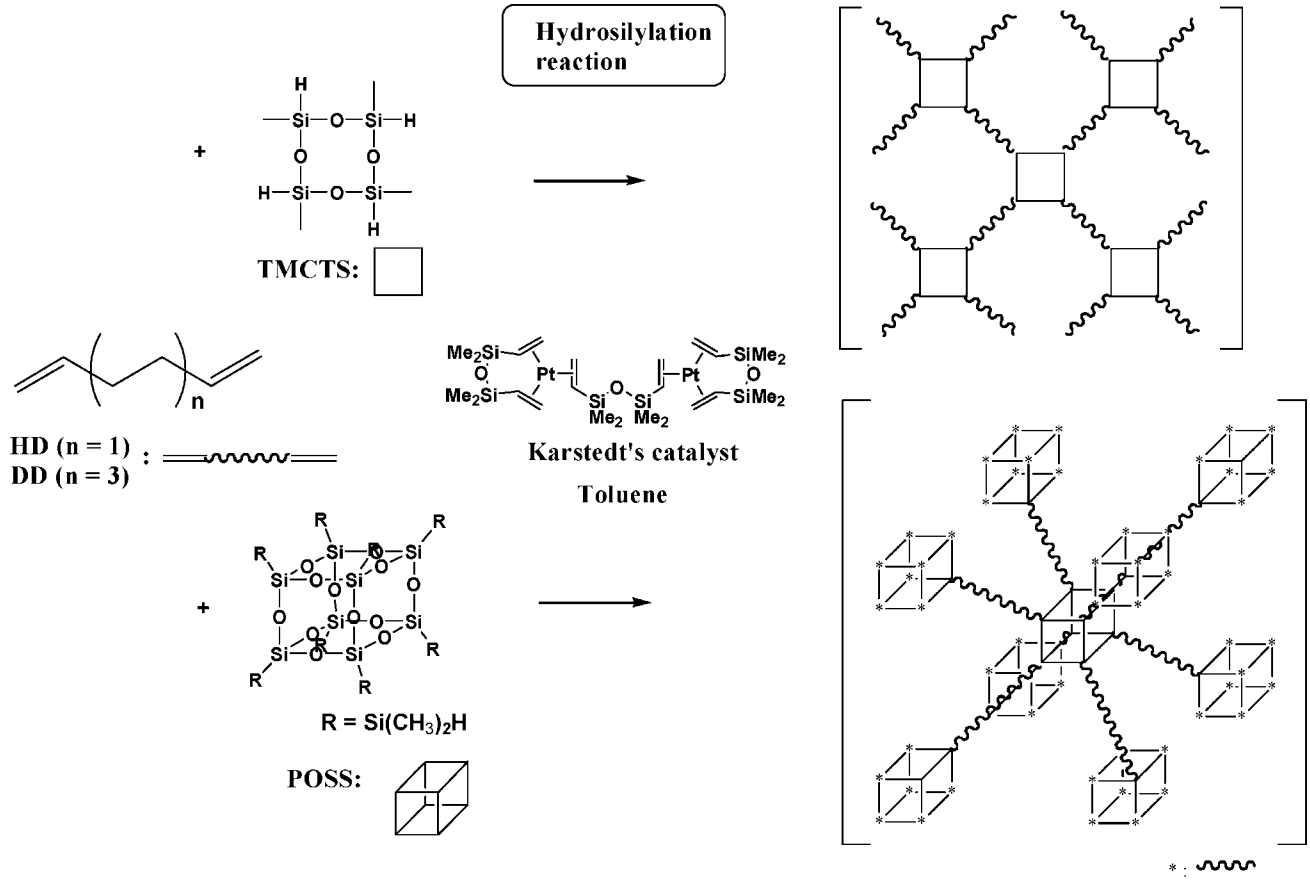

Scheme 2. Photo Hydrosilylation Reaction of TMCTS and POSS with HD and DD Using Bis(acetylacetonato)platinum ($Pt(acac)_2$) Catalyst

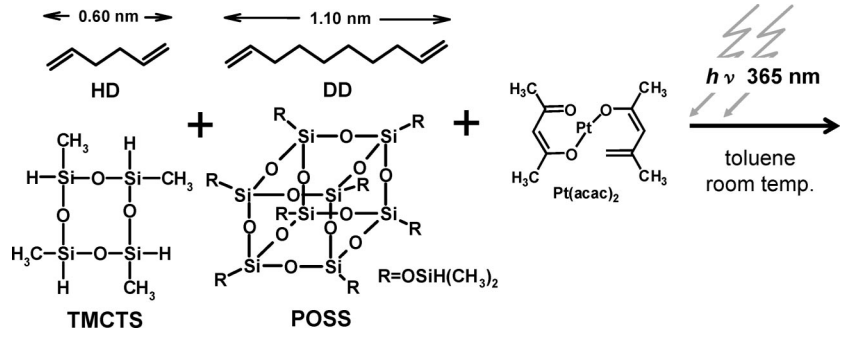

without further purification. $Pt(acac)_2$ was purchased from Wako Pure Chemical Industries and was used without purification. Toluene was dried over calcium hydride under refluxing for 6 h and distilled before use under a nitrogen atmosphere. Boron subphthalocyanine chloride was commercially obtained from Aldrich Chemical and was used as received.

Synthesis of Organic−Inorganic Hybrid Gels by Means of a Photo Hydrosilylation Reaction. The mole ratio of vinyl group in diene to Si−H group in cross-linking reagent was adjusted to 1.0. The molar ratio of vinyl group (or Si−H group) to the Pt catalyst was 1000 in the reaction system. Samples were prepared with special care to get rid of dust and were measured in the as-prepared state in toluene at 25 °C.

Photo Hydrosilylation of TMCTS with HD (Run 7). $Pt(acac)_2$ (0.2 mg, 0.51 μmol), HD (21.4 mg, 0.26 mmol), TMCTS (31.3 mg, 0.13 mmol), and toluene (244 μL) were added to a sample tube of 4 mm diameter under the nitrogen atmosphere, and the catalyst was dissolved with shacking to yield a homogeneous solution. After the sample tube was sealed by burning off, UV light of 365 nm and 1220 W/cm^2 was irradiated for 20 min. The colorless and clear gel was generated. The gels with different monomer concentration or with DD were prepared via the same procedure.

Photo Hydrosilylation of POSS with DD (Run 20). $Pt(acac)_2$ (0.1 mg, 0.25 μmol), DD (8.3 mg, 0.06 mmol), POSS (15.3 mg, 0.015 mmol), and toluene (273 μL) were added to a sample tube of 4 mm diameter under the nitrogen atmosphere, and the catalyst was dissolved with shacking to yield a homogeneous solution. After the sample tube was sealed by burning off, UV light of 365 nm and 1220 W/cm^2 was irradiated for 20 min. The colorless and clear gel was generated. The gels with different monomer concentration or with HD were prepared via the same procedure.

Trace of TMCTS-HD Gel Formation Process with Scanning Microscopic Light Scattering. $Pt(acac)_2$ (0.1 mg, 0.25 μmol), HD (21.4 mg, 0.26 mmol), TMCTS (31.3 mg, 0.13 mmol), and toluene (408 μL) were added to a sample tube of 4 mm diameter under the nitrogen atmosphere (13.0 wt % of monomer concentra-

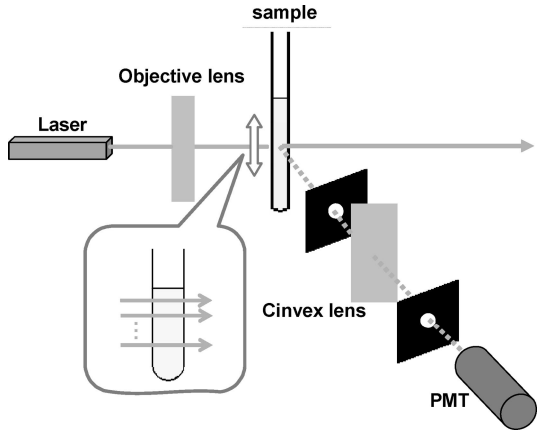

Figure 1. Schematic of scanning microscopic light scattering (SMILS); PMT: photomultiplier tube.

tion), and the catalyst was dissolved with shacking to yield a homogeneous solution. After the sample tube was sealed by burning off, UV light of 365 nm and 790 W/cm^2 was irradiated for 15 min. The sample tube was placed without stirring on the sample stage of SMILS in the dark, and time evolution of the reaction system was investigated with SMILS.

Analytical Procedures. *Scanning Microscopic Light Scattering.* Measuring of mesh size and mesh size distribution of gels gives us quantitative information to design and synthesize the gels with desired network structure. Quantitative determination of minute mesh size of the gels was performed with the SMILS,[37,38] which was recently developed for the detailed characterization of network structure in polymer gels. Because a polymer gel is a huge macromolecule with an infinite network, its characterization should be performed via in situ measurements. In general, conventional dynamic light scattering (DLS) is rarely used to characterize the network structure in polymer gels quantitatively because the static inhomogeneities are memorized in the network. The developed SMILS enables us to perform the DLS measurements at many different positions in an inhomogeneous gel to determine rigorously a time- and space-averaged, that is, ensemble-averaged, (auto-) correlation function of fluctuating mesh size in the gel. The schematic of SMILS is shown in Figure 1, and the fundamentals of SMILS are described below.

A dynamic structure factor $f(\mathbf{q},\tau)$ is determined from the observable properties in DLS studies. $f(\mathbf{q},\tau)$ has the meaning of an autocorrelation function of the density fluctuation in samples, where τ and $\mathbf{q}$ are the correction time and scattering vector, respectively. $f(\mathbf{q},\tau)$ is directly proportional to the first-order autocorrelation function of the scattered electric field, $E(\mathbf{q},\tau)$, as

$$f(\mathbf{q},\tau) \sim \langle E^*(\mathbf{q},t)E(\mathbf{q},t+\tau)\rangle_{en} \propto g_{en}^{(1)}(\mathbf{q},\tau) \tag{1}$$

where $\langle ...\rangle_{en}$ means ensemble-averaging and $g_{en}{}^{(1)}(\mathbf{q},\tau)$ is an ensemble-averaged first-order autocorrelation function of $E(\mathbf{q},\tau)$.[39]

In the case of gels, we should consider a static function built in by the concentration fluctuation during preparation reactions. Such a static fluctuation is inevitably observed by light scattering experiments of usual gels as "speckle pattern", that is, a large static component of scattering intensity that strongly depends on the measuring position in a sample. The position-dependent static fluctuation results in the fact that the time-averaged autocorrelation function obtained at one position of scattering volume, $g_t{}^{(1)}(\mathbf{q},\tau)$, has an anomalous nonrelaxation component called a baseline, which depends on the position of scattering volume in the sample. The ensemble-averaged autocorrelation function, $g_{en}{}^{(1)}(\mathbf{q},\tau)$, obtained by space averaging of a large number of $g_t{}^{(1)}(\mathbf{q},\tau)$ obtained at different positions of scattering volume, also has the nonrelaxation component that is a unique quantity characterizing the sample as a whole. In the present work, the properties of the gel correlation function, $g_{en}{}^{(1)}(\mathbf{q},\tau)$, are explored. In the following, we explain the derivation of $g_{en}{}^{(1)}(\mathbf{q},\tau)$.

Table 1. Constants Used in the Calculations

Boltzmann constant	$k_B = 1.38 \times 10^{-23}$ J K^{-1}
temperature	$T = 303$ K
scattering angle	$\theta = 90°$
wavelength of incident ray	$\lambda = 5.32 \times 10^{-7}$ m
refractive index of toluene	$n = 1.4961$
viscosity coefficient of toluene at 303 K	$\eta = 5.22 \times 10^{-4}$ Nm^{-2} s

The time-averaged first-order autocorrelation function of the scattered electric filed, $E(\mathbf{q},\tau)$, is defined by

$$g_t^{(1)}(\mathbf{q},\tau) \equiv \frac{\langle E^*(\mathbf{q},\tau)E(\mathbf{q},t+\tau)\rangle_t}{(\langle I(\mathbf{q},\tau)\rangle_t\langle I(\mathbf{q},t+\tau)\rangle_t)^{1/2}} \tag{2}$$

where t denotes real time, $I(\mathbf{q},\tau)$ is the scattering intensity at $\mathbf{q}$ and τ, and $\langle ...\rangle_t$ stands for the time-averaging operation.[40] Here "time-averaging" means that the DLS measurement is carried out at one position of scattering volume in the sample and the time average of $E^*(\mathbf{q},\tau)E(\mathbf{q},t+\tau)$ is measured on the laboratory time scale. In the actual measurement with a common self-beating method, we directly measure the time-averaged autocorrelation function of $I(\mathbf{q},\tau)$, that is, the time-averaged second-order autocorrelation function of $E(\mathbf{q},\tau)$, which is defined by[40]

$$g_t^{(2)}(\mathbf{q},\tau) \equiv \frac{\langle I(\mathbf{q},\tau)I(\mathbf{q},t+\tau)\rangle_t}{(\langle I(\mathbf{q},\tau)\rangle_t\langle I(\mathbf{q},t+\tau)\rangle_t)} \tag{3}$$

We need to relate $g_t{}^{(2)}(\mathbf{q},\tau)$ to $g_t{}^{(1)}(\mathbf{q},\tau)$ to determine the dynamic structure factor from $g_t{}^{(2)}(\mathbf{q},\tau)$. There is a known approximate relationship between them called the Gaussian approximation, which can be used if $E(\mathbf{q},\tau)$ is the zero-mean Gaussian variable. This relationship is written as

$$g_{en}^{(2)}(\mathbf{q},\tau) = 1 + \gamma^2[g_{en}^{(1)}(\mathbf{q},\tau)]^2 \tag{4}$$

where γ ($0 \le \gamma \le 1$) is called the coherence factor, which takes into account the incoherence effect arising from the finite area of the detector. Under an ideal condition, $\gamma = 1$.[39] This ideal condition is commonly used in DLS analysis and is known as the Siegert relationship. In the case of gels, however, this equation cannot be used because actual gels usually have static inhomogeneities so that the time average is not zero, that is, $\langle E(\mathbf{q},\tau)\rangle_t \neq 0$. We use the extended version of the Siegert relationship for the gels containing inhomogeneity as the following equation

$$g_t^{(2)}(\mathbf{q},\tau) = 1 + \gamma^2[g_t^{(1)}(\mathbf{q},\tau)]^2 - \gamma^2[g_t^{(1)}(\mathbf{q},\infty)]^2 \tag{5}$$

or

$$g_t^{(1)}(\mathbf{q},\tau) = \gamma^{-1}\sqrt{1 + g^{(2)}(\mathbf{q},\tau) - g^{(2)}(\mathbf{q},0)} \tag{6}$$

In the case of homogeneous media, $g_t{}^{(1)}(\mathbf{q},\infty) = 0[g_t{}^{(2)}(\mathbf{q},0) = 2]$, and eq 5 reduces to eq 4.[41]

As mentioned above, the ensemble-average correction function, $g_{en}{}^{(1)}(\mathbf{q},\tau)$, should be determined to obtain the dynamic structure factor corresponding to the sample as a whole while taking into account the position dependence of $g_t{}^{(1)}(\mathbf{q},\tau)$ due to the inhomogeneities of gels.[42] In actual measurements, $g_{en}{}^{(1)}(\mathbf{q},\tau)$ is calculated as the space average of the time-averaged correlation function as

$$g_{en}^{(1)}(\mathbf{q},\tau) \equiv \frac{\langle E^*(\mathbf{q},\tau)E(\mathbf{q},t+\tau)\rangle_{en}}{(\langle I(\mathbf{q},\tau)\rangle_{en}\langle I(\mathbf{q},t+\tau)\rangle_{en})^{1/2}}$$

$$= \frac{\langle\langle E^*(\mathbf{q},\tau)E(\mathbf{q},t+\tau)\rangle_t\rangle_{sp}}{\langle I(\mathbf{q},\tau)\rangle_{en}} \tag{7}$$

where $\langle ...\rangle_{sp}$ means space-averaging operation. By using eqs 2 and 6, we obtain

$$g_{en}^{(1)}(\mathbf{q},\tau) = \frac{\langle\langle I(\mathbf{q},\tau)\rangle_t g_t^{(1)}(\mathbf{q},\tau)\rangle_{sp}}{\langle I(\mathbf{q},\tau)\rangle_{en}} = \frac{\langle\langle I(\mathbf{q},\tau)\rangle_t \gamma^{-1}\sqrt{1 + g_t^{(2)}(\mathbf{q},\tau) - g_t^{(2)}(\mathbf{q},0)}\rangle_{sp}}{\langle I(\mathbf{q},\tau)\rangle_{en}} \quad (8)$$

It should be noted that $g_{en}^{(1)}(\mathbf{q},\tau) \neq \langle g_{en}^{(1)}(\mathbf{q},\tau)\rangle_{sp}$. Therefore, we should use eq 8 to calculate $g_{en}^{(1)}(\mathbf{q},\tau)$.[42]

If one focuses only on the dynamic component of the dynamic structure factor, that is, on the dynamics of the inhomogeneous media, then the normalized dynamic component of $g_{en}^{(1)}(\mathbf{q},\tau)$ can be calculated by

$$\Delta g_{en}^{(1)}(\mathbf{q},\tau) = \frac{g_{en}^{(1)}(\mathbf{q},\tau) - g_{en}^{(1)}(\mathbf{q},\infty)}{g_{en}^{(1)}(\mathbf{q},0) - g_{en}^{(1)}(\mathbf{q},\infty)} = \frac{\langle\langle I(\mathbf{q},\tau)\rangle_t\sqrt{1 + g_t^{(2)}(\mathbf{q},\tau) - g_t^{(2)}(\mathbf{q},0)}\rangle_{sp} - \langle\langle I(\mathbf{q},\tau)\rangle_t\sqrt{2 - g_t^{(2)}(\mathbf{q},0)}\rangle_{sp}}{\langle I(\mathbf{q},\tau)\rangle_{en} - \langle\langle I(\mathbf{q},\tau)\rangle_t\sqrt{2 - g_t^{(2)}(\mathbf{q},0)}\rangle_{sp}} \quad (9)$$

This equation is free from γ. It means that the incoherent effect does not need to be taken care of in the analysis of dynamics by using eq 9.

Furthermore, by using the baseline of $g_{en}^{(1)}(\mathbf{q},\tau)$, we can separately obtain the static and the dynamic components, $\langle I_s(\mathbf{q})\rangle_{en}$ and $\langle I_d(\mathbf{q})\rangle_{en}$, of the ensemble-averaged scattering intensity, $\langle I(\mathbf{q},t)\rangle_{en}$. We find that the heterodyne function, $g_{en}^{(1)}(\mathbf{q},\tau)$, has a "baseline" due to the presence of the static fluctuation. Therefore, we obtain the following equations[42,43]

$$\langle I_s(\mathbf{q})\rangle_{en} = \langle I(\mathbf{q},t)\rangle_{en} g_{en}^{(1)}(\mathbf{q},\infty) \quad (10)$$

$$\langle I_d(\mathbf{q},t)\rangle_{en} = \langle I(\mathbf{q},t)\rangle_{en}[1 - g_{en}^{(1)}(\mathbf{q},\infty)] \quad (11)$$

By using the above formulas for $g_{en}^{(1)}(\mathbf{q},\tau)$, $\Delta g_{en}^{(1)}(\mathbf{q},\tau)$, $\langle I_s(\mathbf{q})\rangle_{en}$, and $\langle I_d(\mathbf{q})\rangle_{en}$, we are able to characterize all of the properties of the inhomogeneous medium, even when it has a nonergodic nature. In particular, as described below, we can calculate an ensemble-averaged distribution function, $P_{en}(\mathbf{q},\tau_R)$, of relaxation time, τ_R, directly from $\Delta g_{en}^{(1)}(\mathbf{q},\tau)$ by using a kind of inverse Laplace transform method. Such a $P_{en}(\mathbf{q},\tau_R)$ gives full information on the dynamic fluctuation of the media. In the case of polymer gels, for instance, distributions of mesh size, cluster radius, and son on are obtained.Furthermore, from $\langle I_s(\mathbf{q})\rangle_{en}$ and $\langle I_d(\mathbf{q})\rangle_{en}$, we can obtain valuable information on static and dynamic inhomogeneities in polymer gels. These are intrinsic merits of using the above equations.

In the present work, the dynamic component of the ensemble-averaged correlation function, $g_{en}^{(1)}(\mathbf{q},\tau)$, was analyzed with a kind of inverse Laplace transform method, as mentioned above. In general, $g_{en}^{(1)}(\mathbf{q},\tau)$ can be approximately expressed by a superposition of many exponential functions as

$$\Delta g_{en}^{(1)}(\mathbf{q},\tau) = \sum_{i=0}^{n} P(\tau_{R,i}) \exp\left(-\frac{\tau}{\tau_{R,i}}\right) \quad (12)$$

where $\{\tau_{R,i}\}$ is a geometric progression of relaxation time expressed as[44,45]

$$\tau_{R,i} = \tau_{R,max}(\tau_{R,max}/\tau_{R,min})^{(i-1)/n} \; (i = 1, 2, n) \quad (13)$$

The radius of mesh in Brownian motion can be estimated by the following eq 15, which is derived from the ensemble-averaged correlation function, equation of diffusion coefficient eq 14, and Einstein−Stokes formula.

$$\frac{1}{\tau_R} = \mathbf{q}^2 D_{coop} \quad (14)$$

$$D_{coop} \cong \frac{k_B T}{6\pi\eta\xi} \quad (15)$$

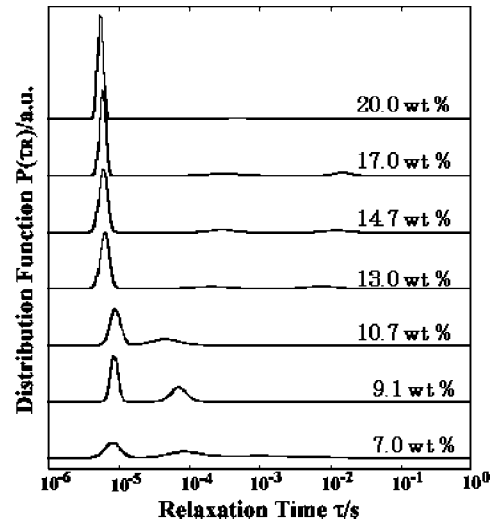

Figure 2. Ensemble-averaged relaxation-time distribution as a function of the relaxation time of TMCTS-HD gels.

where D_{coop}, k_B, T, η, and ζ are the cooperative diffusion coefficient, Boltzmann constant, temperature, viscosity coefficient of solvent, and radius of mesh (m), respectively.

The observed modes, as assigned to the cooperative diffusion of gel network, are used to determine the radius of mesh (mesh size) (ξ; m) as eq 16 in this experiment

$$\zeta = d \approx \frac{16\pi n^2 \tau_R k_B T \sin^2\frac{\theta}{2}}{3\eta\lambda^2} \quad (16)$$

where n, τ_R, θ, η, and λ are the refractive index of toluene, ensemble-averaged relaxation time, scattering angle, viscosity coefficient of toluene, and wavelength of the incident ray, respectively. The constants used in these calculations are summarized in Table 1.

Scanning measurements were performed at more than 25 points for each sample to determine the ensemble-averaged dynamic structure factor. For these gels, a few peaks of relaxation modes were observed in the distribution function.[32,33] On the basis of the observation of scattering angle, q, dependence of the relaxation modes, all of the observed modes usually have q^2 dependence, which corresponds to translational diffusion. In the following, all of the results were determined at a scattering angle fixed at 90°.

^{1}H NMR spectra of sol samples, not gel samples, were recorded on a JEOL-JNM-LA300 spectrometer in pulse Fourier transform mode. The pulse angle was 45°, and 32 scans were accumulated in 7 s of the pulse repetition. The spectra were recorded at room temperature with C_6D_6.

Results and Discussion

The photo hydrosilylations of TMCTS with HD were investigated with $Pt(acac)_2$ under various monomer concentrations in toluene (Scheme 2). Formation of the gel was confirmed by the absence of fluidity of the reaction system. The gels were obtained in the reaction at monomer concentrations of >6.5 wt % (wt % of summation of TMCTS and HD in the reaction system). However, viscous liquids were generated with less than this monomer concentration. We will use the term of "critical gelation concentration" to refer the lowest monomer concentration that generates a gel.

Figure 2 shows the ensemble-averaged relaxation time distributions as a function of the relaxation time of TMCTS-HD gels, which were prepared at various monomer concentrations. The structure of the mesh is summarized in Table 2. Bimodality was detected in ensemble-averaged relaxation time

Table 2. Structures of TMCTS-HD and -DD Gels Prepared with $Pt(acac)_2$

run	diene	monomer concentration (wt %)	$\tau_R \times 10^{-6}$ (s)[a]	σ[b]	mesh size (nm)
1	HD	7.0	8.1	0.12	2.2
			82.7	0.24	22.0
2	HD	9.1	8.5	0.056	2.3
			70.6	0.12	18.7
3	HD	10.7	8.8	0.079	2.3
			45.2	0.20	12.1
4	HD	13.0	6.2	0.065	1.7
5	HD	14.7	5.9	0.060	1.6
6	HD	17.0	5.8	0.044	1.5
7	HD	20.0	5.4	0.039	1.4
8	DD	4.3	5.3	0.24	1.4
			135	0.49	36.1
9	DD	5.7	4.7	0.14	1.3
			65.4	0.093	17.4
10	DD	7.4	5.5	0.053	1.5
			115	0.093	30.5
11	DD	9.1	6.2	0.043	1.6
			393	0.075	104

[a] Relaxation time. [b] Standard deviation of a peak of the ensemble-averaged relaxation time distribution.

Table 3. Structures of POSS-HD and -DD Gels Prepared with $Pt(acac)_2$

run	diene	monomer concentration (wt %)	$\tau_R \times 10^{-6}$ (s)[a]	σ[b]	mesh size (nm)
12	HD	10.7	5.9	0.12	1.6
			39.9	0.20	10.6
13	HD	13.0	5.4	0.077	1.4
			44.0	0.14	11.7
14	HD	14.7	5.1	0.073	1.4
			73.9	0.10	19.6
15	HD	17.0	4.5	0.063	1.2
			73.3	0.092	19.4
16	HD	20.0	5.4	0.056	1.4
17	HD	22.0	5.3	0.16	1.4
18	DD	5.7	6.6	0.055	1.8
			98.1	0.20	26.0
19	DD	7.4	5.9	0.061	1.6
20	DD	9.1	5.4	0.060	1.4
			52.6	0.089	14.0

[a] Relaxation time. [b] Standard deviation of a peak of the ensemble-averaged relaxation time distribution.

distributions in the gels generated from low monomer concentrations (7.0−10.7 wt %), which were a little higher than the critical gel concentration. The peaks at short relaxation time ($<10^{-5}$ s) correspond to mesh sizes of about 1.5 nm. The model of the mesh of TMCTS-HD gel is shown in Scheme 3. The mesh size is close to the calculated (molecular mechanics method) mesh size derived from TMCTS and HD (0.9 nm). In our previous report, similar mesh size was detected in the TMCTS-HD gels prepared with Karstedt's catalyst.[32] We concluded that the small mesh was derived from TMCTS and HD. However, the peaks at long relaxation time (at around 10^{-4} s) correspond to the mesh size of 12−22 nm, which is about ten times greater than the mesh size derived from TMCTS and HD. The structure of the large mesh would be a defect in the network derived from vacant space between micro gels. This is a question to be considered later in the experiment of the gel formation process. The bimodal relaxation peaks demonstrate inhomogeneity of the network structure. However, the gels generated at relatively high monomer concentrations (13.0 to 20.0 wt %) showed a unimodal distribution of the ensemble-averaged relaxation time. The relaxation time derived from the small mesh decreased with increasing monomer concentration. Furthermore, the minimum value of σ, which corresponds to mesh size distribution, was achieved in the gel of 20.0 wt % of monomer concentration. The gels prepared at more than 20.0 wt % of monomer concentration formed cracks, bubbles, or both in the gels because of the reaction heat and repulsion derived from the excluded volume effect between the molecules of mesh. These results indicate that the most suitable monomer concentration for the homogeneous network is 20.0 wt %. The monomer concentration that produces the gels having the minimum mesh size and a narrow mesh size distribution is applied to the following investigations as the "optimal gelation concentration".

The photo hydrosilylation reaction of TMCTS with DD and POSS with HD or DD has also been investigated in the same way. The structure of the gels is summarized in Tables 2 and 3. The critical gelation concentrations of TMCTS-DD, POSS-HD, and POSS-DD gels were 4.3 wt %, 10.7 wt %, and 5.7 wt %, respectively, summarized in Table 4. The gels generated at low monomer concentrations, which were a little higher than the critical gelation concentration, show bimodality in the ensemble-averaged relaxation time distributions. The optimal gelation concentrations of TMCTS-DD, POSS-HD, and POSS-DD gels were 9.1 wt % (run 11), 20.0 wt % (run 16), and 7.4 wt % (run 19), respectively. The gels with DD showed lower critical gelation concentration than those with HD. The ensemble-averaged relaxation time of the gels synthesized at the optimal gelation concentration is illustrated in Figure 3. The Figure demonstrates that mesh size of the gels with DD is larger than

Scheme 3. Schematic of Mesh of TMCTS-HD Gel

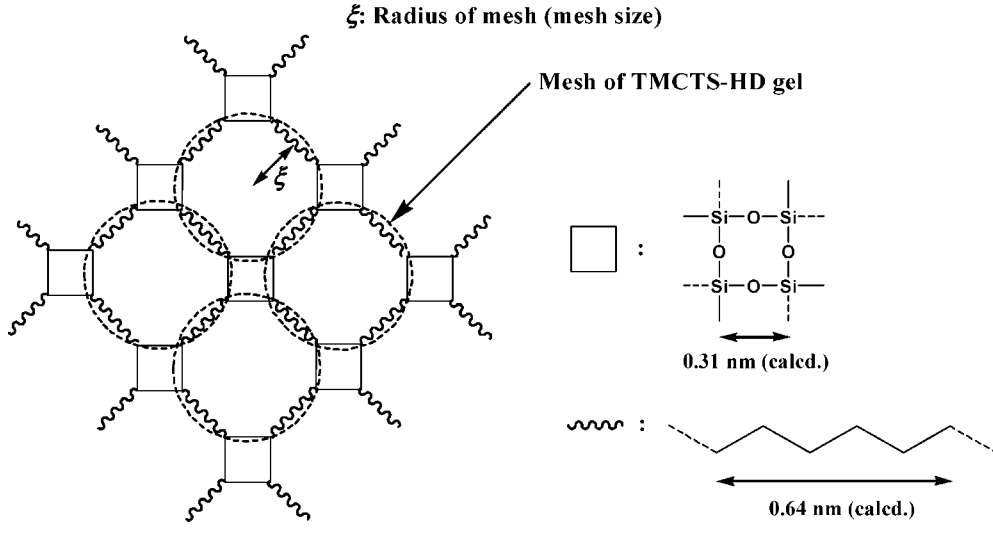

Table 4. Results of Photo Hydrosilylation Reaction, Gelation of TMCTS and POSS with HD and DD

	sol state		critical gelation	optimal gelation	
monomer composition	monomer concentration (wt %)	reaction conversion (%)[a]	monomer concentration (wt %)	monomer concentration (wt %)	gelation time (min)
TMCTS-HD	5.7	86	6.5	20.0	immediate
TMCTS-DD	2.4	86	4.3	9.1	immediate
POSS-HD	9.0	90	10.7	20.0	10
POSS-DD	4.2	97	9.1	7.4	20

[a] Determined by ^{1}H NMR.

that of the gels with HD; to put it another way, the molecular length of the nonconjugated diene reflects the mesh size of the resulting gels. The relaxation time distributions of the gels with HD are quite narrow, whereas the relaxation time distributions of the gels with DD have a few weak relaxation peaks with an intense main relaxation peak. The σ values, which correspond to the mesh size distribution, of the gels with POSS are higher than those with TMCTS. The reaction conversions of the photo hydrosilylation in the sol sample, which was prepared at lower monomer concentration than the critical gelation concentration, were investigated with ^{1}H NMR spectroscopy after 20 min of the UV irradiation. The results are summarized in Table 4 together with the critical gelation concentration. The reaction conversions are high enough to form the network structure, and the reaction conversions with POSS (90−97%) are a little higher than those with TMCTS (87%). The difference of the reaction conversion between POSS and TMCTS should be derived from the difference in mobility of the Si−H group. The Si atoms of Si−H groups in TMCTS are included in the cyclic siloxane, whereas those in POSS are connected to cubic silsesquioxane with oxygen. The Si−H groups in POSS should have higher mobility than those in TMCTS. Although the reaction conversions with POSS are higher than those with TMCTS, the critical gelation concentration of the gels with POSS is lower than that of the gels with TMCTS. The σ values of the gels with POSS were larger than those of the gels with TMCTS. Furthermore, it took a longer time to form the gels with POSS than the gels with TMCTS in comparison with the optimal gelation concentration (Table 4). Plausible models of formation of the TMCTS-HD gel and POSS-HD gel are shown in Scheme 4 to explain these unexpected results. When the concentration of "cross-linking points" (Si−H group) is compared in the same monomer concentration, the concentration of the cross-linking points in the TMCTS-HD gel is higher than those in the POSS-HD gel; for example, 1.03 mol/L for TMCTS-HD gel and 0.82 mol/L for POSS-HD gel at 10.7 wt % of the monomer concentration. In addition, not only an ideal reaction to form the homogeneous network but also unexpected reactions to induce defects in the network, such as intramolecular cross-linking, should occur in the hydrosilylation reaction of POSS and HD because of the side effects of Si−H groups having high mobility and high reaction conversions of the reaction system, as shown in Scheme 4. These factors should induce high critical gelation concentration, bimodal or broad distribution of the mesh size, and long gelation time of the gels with POSS.

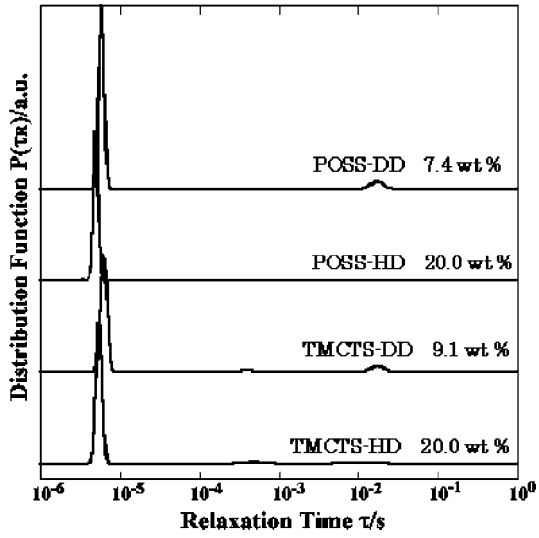

Figure 3. Ensemble-averaged relaxation-time distribution as a function of the relaxation time of the gels synthesized at optimal gelation concentration.

The structures of the corresponding gels previously prepared with the platinum−divinyltetramethyldisiloxane complex (Karstedt's catalyst)[32] are compared with those gels obtained in the present study. Even though a few weak relaxation peaks derived from the inhomogeneity of the network structures are detected in the gels with DD, the gels prepared with $Pt(acac)_2$ show quite narrow size distributions and almost presupposed (calculated) mesh size. TMCTS-DD and POSS-DD gels prepared with Karstedt's catalyst showed bimodal or multimodal distributions of mesh size because of the frequent unexpected intermolecular cross-linking and intramolecular cyclization of DD, as previously reported. Figure 4 shows the relationship between the stretched diene length and mesh size of the gels with TMCTS obtained using $Pt(acac)_2$ or Karstedt's catalysts. Both of the catalysts produced TMCTS-HD gels having close to the calculated mesh size with homogeneous distribution. However, Karstedt's catalyst yielded the TMCTS-DD gels having much larger mesh size than the calculated size with bimodal distribution. The latter result shows that $Pt(acac)_2$ catalyst is superior to Karstedt's catalyst for the formation of the present organic−inorganic hybrid gels with homogeneous network structure. The homogeneous distribution in the reaction system without proceeding of the reaction and simultaneous initiation of the reaction with UV irradiation throughout the reaction system with $Pt(acac)_2$ catalyst should induce the formation of the homogeneous and ideal network.

The formation process of the TMCTS-HD gel, prepared under the conditions described in the Experimental Part, has been traced with SMILS. Time evolution of the time-averaged relaxation-time distribution as a function of the relaxation time is shown in Figure 5, and corresponding mesh sizes are summarized in Figure 6. The gel was generated after between 4.5 and 5.0 h from the UV irradiation in this experiment. A sharp relaxation peak detected at $<10^{-5}$ s in the reaction system immediately at (Figure 5c) and after 1.0 h (Figure 5d) from the irradiation should be derived from toluene, monomers, or both (Figures 5a,b). A somewhat broad relaxation peak derived from TMCTS-HD mesh appeared at around 10^{-5} s after 2 h from the irradiation (Figure 5e). This mesh size decreased with increasing reaction time until the gel formation, as observed in Figure 5f−h and Figure 6a. When the reaction was nearing the gelation point, mesh size decreased, and the mesh size distribution becomes narrow. The most likely explanation is that the reaction of TMCTS with HD has proceeded enough to occupy all of the space in the gel with the mesh and has formed the expected network structure of highly dense mesh with small size. However, the mesh size of the gel slightly increased after the gelation (Figures 6h−j). Although, there is room for further investigation, one explanation for the result is that the mesh in the gel would not reach the equilibrium structure immediately after the gelation. It would take a few hours to reach the equilibrium by expansion of the tightly formed mesh in the gel.

In the early stage of the reaction, the network formation is imperfect to form the gel, and the network has the defect of large mesh and shows broad distribution of the mesh size. A

Scheme 4. Proposed Network Structure of TMCTS-HD or POSS-HD Gels

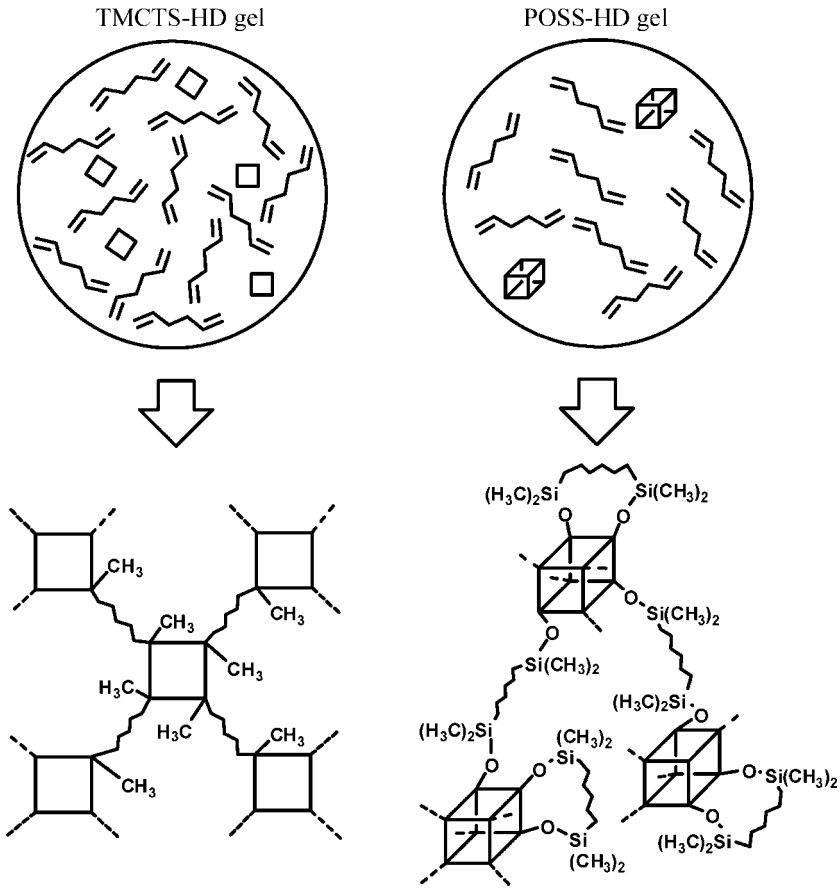

weak relaxation peak was detected at 10^{-3} to 10^{-4} s, which corresponds to 26−65 nm of the mesh, during 1−4 h after the irradiation (Figure 5d−g). The relaxation time decreased with increasing reaction time, as shown in Figure 6b, and disappeared at around the gelation point. This mesh size is much larger than that of the presupposed mesh size from TMCTS-HD, as described above. The proposed formation mechanism of the TMCTS-HD gel is shown in Scheme 5. One explanation for the large mesh size may be derived from the vacant space between micro gels. The micro gels would be formed isolated in the early stage of the reaction. As the reaction is proceeding,

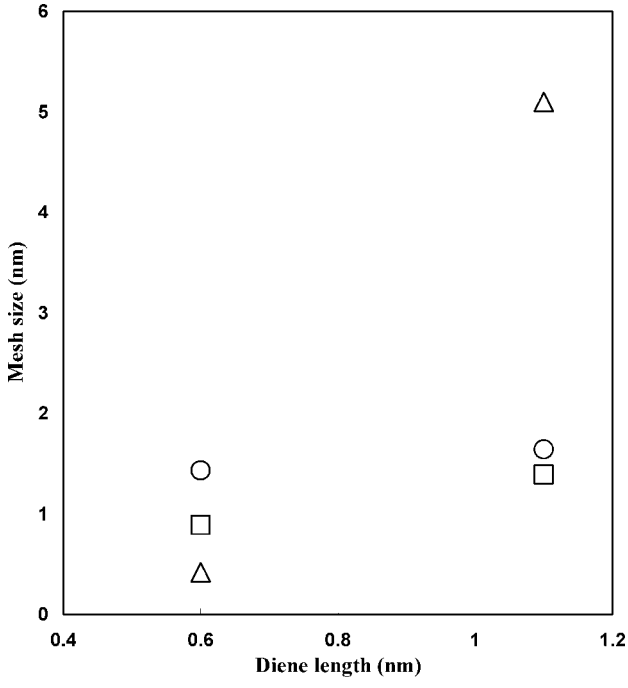

Figure 4. Relationship between the stretched diene length (HD, 0.60 nm; DD, 1.1 nm) and mesh size of the gels with TMCTS obtained with $Pt(acac)_2$ catalyst (○), Karstedt's catalyst (△), and calculated mesh size (□).

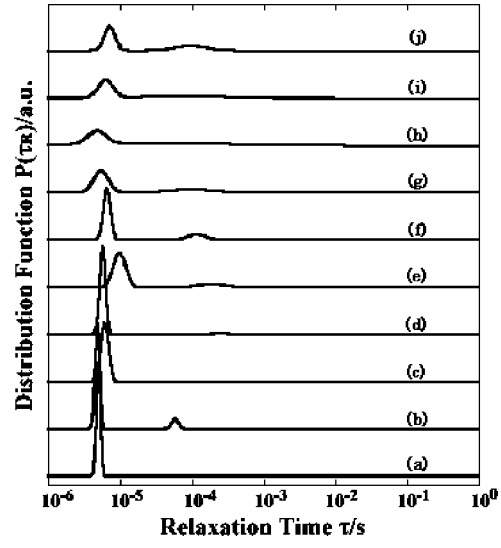

Figure 5. Time-averaged relaxation-time distribution as a function of the relaxation time of TMCTS-HD gelation process: (a) toluene, (b) before irradiation, (c) immediately after irradiation, (d) after 1 h, (e) after 2 h, (f) after 3 h, (g) after 4 h, (h) after 4.5 h, (i) after 5 h, and (j) after 5.5 h from UV irradiation.

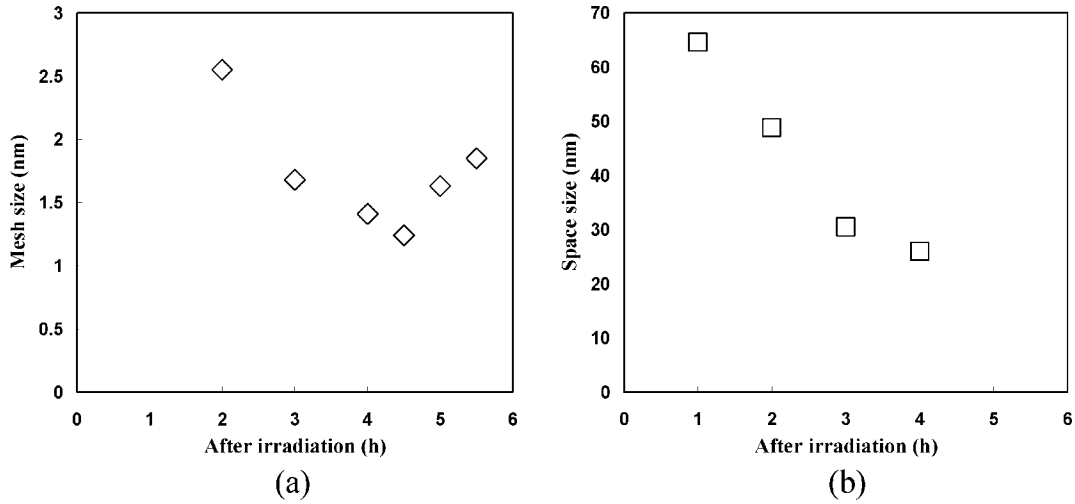

Figure 6. Time evolution of (a) mesh size of small mesh and (b) space size between micro gels in the formation of TMCTS-HD gel.

Scheme 5. Proposed Gelation Mechanism of TMCTS-HD Gel

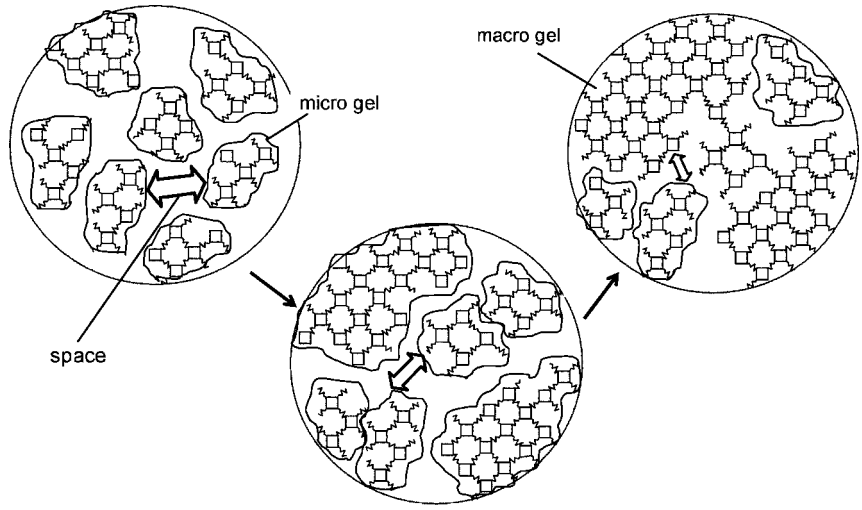

the space will be occupied with aggregation of growing micro gels, newly formed mesh, or both.

The POSS-DD gel (monomer concentration, 7.4 wt %) has been prepared in a small schale (diameter = 2 cm), of which the bottom was covered with photo musk (0.5 × 0.5 cm^2 square, Figure 7), under the same conditions as those in the experimental part of run 20. A red dye of boron subphthalocyanine chloride (SubPC; 1 mg/ml) was added to the reaction medium to color the gel. After the reaction, the reaction medium in the schale was washed with a small amount of toluene to remove the unreacted monomers. Figure 7 shows a photograph of the resulting gel. The gel was formed in the UV irradiated area. In

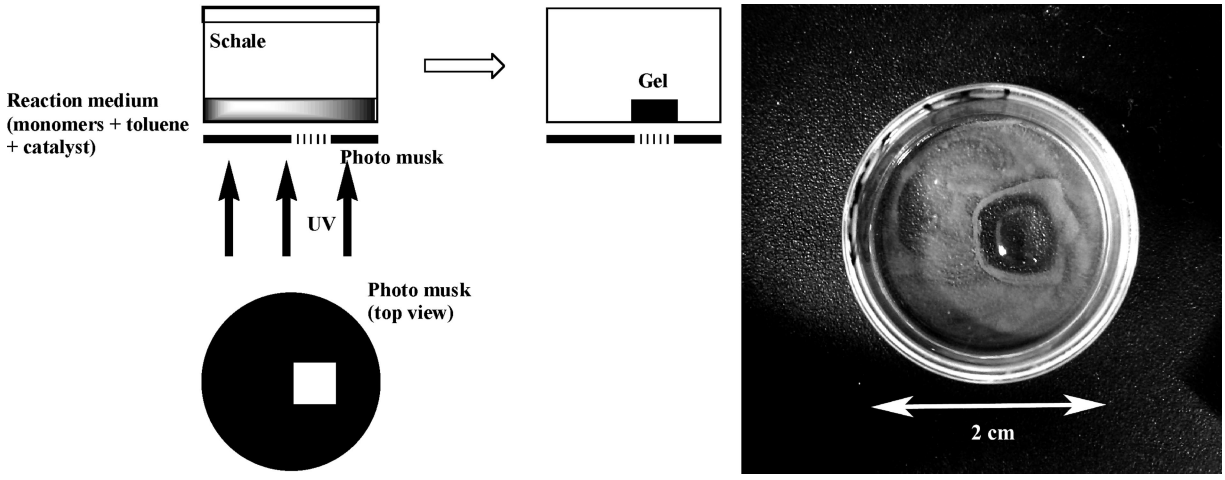

Figure 7. Illustration and photograph of a photo-pattern coating of glass (schale) with the POSS-DD gel containing SubPC.

other words, the photo-pattern coating of glass with the gel is possible by means of this photo hydrosilylation reaction.

Conclusions

Organic−inorganic hybrid gels from TMCTS or POSS with HD or DD have been synthesized by means of a photo hydrosilylation reaction with $Pt(acac)_2$. The use of the $Pt(acac)_2$ catalyst has made remarkable progress in precise synthesis, study of the gelation process, and application possibilities of the organic−inorganic hybrid gels, in comparison with the corresponding synthesis with Karstedt's catalyst previously used. First, photo hydrosilylation reaction has made it possible to produce extremely narrow mesh-size distribution. The corresponding gels with homogeneous mesh-size were successfully obtained in the reaction with HD. Although the gels with DD contained a small part of structure defects in the mesh, improvement in homogenization of mesh size distribution has been attained by means of the photo hydrosilylation reaction. Second, we have traced the formation process of TMCTS-HD gel successfully by means of SMILS. The mesh size transition during the formation of TMCTS-HD gel indicates the formation of micro gels in the early stage of the reaction with large vacant space, and following aggregation of the micro gels, further formation of the mesh, or both would cause the gelation. The reaction with Karstedt's catalyst was too fast to trace the formation of the gel with SMILS. Third, the photo hydrosilylation reaction has successfully applied the photo-pattern coating of a glass with the organic−inorganic gel. The photo-patterned gel coating was formed in the UV irradiated area. The present $Pt(acac)_2$ catalyst has advantages of homogeneous distribution in the reaction system without proceeding of the reaction and simultaneous initiation of the reaction with UV irradiation throughout the reaction system.

The synthesis of the organic−inorganic hybrid gels by means of the photo hydrosilylation reaction should be a superior method not only to form the mesh size of the gels with homogeneous network structure but also to extend the application of the gels, for example, coating a wide area or sealing a narrow gap with the gels. These applications of the organic−inorganic hybrid gels obtained with the photo hydrosilylation reaction are proceeding and will be reported elsewhere.

References and Notes

(1) *Hybrid Organic-Inorganic Composites*; Mark, J. E., Lee, Y.-C. C., Bianconi, P. A. Eds.; ACS Symposium Series 585; American Chemical Society: Washington, DC, 1995.
(2) Mascia, L. *Trends Polym. Sci.* **1995**, *3*, 61.
(3) Novak, B. M. *Adv. Mater.* **1993**, *5*, 442.
(4) Provatas, A.; Matisons, J. G. *Trends Polym. Sci.* **1997**, *5*, 32.
(5) Laine, R. M.; Zhang, C.; Sellinger, A.; Viculis, L. *Appl. Organomet. Chem.* **1998**, *12*, 715.
(6) Vaia, R. A.; Ishi, H.; Giannelis, E. P. *Chem. Mater.* **1996**, *8*, 1728.
(7) Weimer, M. W.; Chen, H.; Giannelis, E. P.; Sogah, D. Y. *J. Am. Chem. Soc.* **1999**, *121*, 1615.
(8) Saegusa, T.; Chujo, Y. *Makromol. Chem., Macromol. Symp.* **1991**, *51*, 1.
(9) Landry, C. J. T.; Coltrain, B. K.; Landry, M. R.; Long, V. K. *Macromolecules* **1993**, *26*, 3702.
(10) Yamada, N.; Yoshinaga, I.; Katayama, S. *J. Mater. Chem.* **1997**, *7*, 1491.
(11) Kim, K. M.; Chujo, Y. *J. Mater. Chem.* **2003**, *13*, 1384.
(12) Choi, J.; Yee, A. F.; Laine, R. M. *Macromolecules* **2003**, *36*, 5666.
(13) Galiastsatos, V.; Subramanian, P.; Klein-Castner, L. *Macromol. Symp.* **2001**, *171*, 97.
(14) Voronkov, M. G.; Lavrentlyev, V. I. *Top. Curr. Chem.* **1982**, *102*, 199–236.
(15) Lichtenhan, J. D.; Vu, H. Q.; Carter, J. A.; Gilman, J. W.; Feher, F. J. *Macromolecules* **1993**, *26*, 2141–2142.
(16) Michalczyk, M. J.; Farneth, W. E.; Vega, A. *J. Chem. Mater.* **1993**, *5*, 1687.
(17) Baney, R. H.; Itoh, M.; Sakakibara, A.; Suzuki, T. *Chem. Rev.* **1995**, *95*, 1409–1430.
(18) Loy, D. A.; Shea, K. *J. Chem. Rev.* **1995**, *95*, 1431–1442.
(19) Provatas, A.; Matisons, J. G. *Trends Polym. Sci.* **1997**, *5*, 327–333.
(20) Zhang, C.; Babonneau, F.; Bonhomme, C.; Laine, R. M.; Soles, C. L.; Hristov, H. A.; Yee, A. F. *J. Am. Chem. Soc.* **1998**, *120*, 8380.
(21) Laine, R. M.; Zhang, C.; Sellinger, A.; Viculis, L. *Appl. Organomet. Chem.* **1998**, *12*, 715.
(22) Tsumura, M.; Ando, K.; Kotani, J.; Hiraishi, M.; Iwahara, T. *Macromolecules* **1998**, *31*, 2716.
(23) Tsumura, M.; Iwahara, T. *Polym. J.* **1999**, *31*, 452.
(24) Tsumura, M.; Iwahara, T. *Polym. J.* **2000**, *32*, 567.
(25) Tsumura, M.; Iwaara, T. *J. Appl. Polym. Sci.* **2000**, *78*, 724.
(26) Auner, N.; Bats, J. W.; Katsoulis, D. E.; Suto, M.; Tecklenburg, R. E.; Zank, G. A. *Chem. Mater.* **2000**, *12*, 3402–3418.
(27) Redondo, S. U. A.; Radovanovic, E.; Torriani, I. L.; Yoshida, I. V. P. *Polymer* **2001**, *42*, 1319.
(28) Pan, G.; Mark, J. E.; Schaefer, D. W. *J. Polym. Sci., Part B: Polym. Phys.* **2003**, *41*, 3314.
(29) Su, R. Q.; Müller, T. E.; Procházka, J.; Lercher, J. A. *Adv. Mater.* **2004**, *14*, 1369.
(30) Pinho, R. O.; Radovanovic, E.; Torriani, I. L.; Yshida, I. V. P. *Eur. Polym. J.* **2004**, *40*, 615.
(31) Laine, R. M. *J. Mater. Chem.* **2005**, *15*, 3725–3744.
(32) Naga, N.; Oda, E.; Toyota, A.; Horie, K.; Furukawa, H. *Macromol. Chem. Phys.* **2006**, *207*, 627–635.
(33) Naga, N.; Oda, E.; Toyota, A.; Furukawa, H. *Macromol. Chem. Phys.* **2007**, *208*, 2331–2338.
(34) Lewis, F. D.; Salvi, G. D. *Inorg. Chem.* **1995**, 3182–3189.
(35) Lewis, F. D.; Mikker, A. M.; Salvi, G. D. *Inorg. Chem.* **1995**, 3173–3181.
(36) Wang, F.; Kaafarani, B. R.; Neckers, D. C. *Macromolecules* **2003**, *36*, 8225–8230.
(37) Furukawa, H.; Horie, K.; Nozaki, R.; Okada, M. *Phys. Rev. E* **2003**, *68*, 031406−1.
(38) Furukawa, H.; Kobayashi, M.; Miyashita, Y.; Horie, K. *High Perform. Polym.* **2006**, *18*, 837–847.
(39) Berne, B. J.; Precora, R. *Dynamic Light Scattering: with Applications to Chemistry, Biology, And Physics*; Wiley: New York, 1976.
(40) Loudon, R. *The Quantum Theory of Light*, 3rd ed.; Oxford University Press: Oxford, 2001.
(41) Pusey, P. N.; van Megen, W. *Physica A* **1989**, *157*, 705.
(42) Furukawa, H.; Hirotsu, S. *J. Phys. Soc. Jpn.* **2002**, *71*, 2873.
(43) Geissler, E.; Horkay, F.; Hecht, A. H. *J. Chem. Phys.* **1995**, *102*, 9129.
(44) McWhirter, J. G.; Pike, E. R. *J. Phys. A: Math. Gen.* **1978**, *11*, 1729.
(45) Ostrowsky, N.; Sornette, D.; Parker, P.; Pike, E. R. *Opt. Acta* **1981**, *28*, 1059.

MA802745X